UDC 539.3

# TUNING OF VIBRO-IMPACT NONLINEAR ENERGY SINKS UNDER CHANGING STRUCTURAL PARAMETERS. PART 2. COMPARISON WITH TUNED MASS DAMPERS

**P.P. Lizunov**

**O.S. Pogorelova**

**T.G. Postnikova**

*Kyiv National University of Construction and Architecture*
*31, Povitryanykh Sylave., Kyiv, Ukraine, 03680*

DOI: 10.32347/2410-2547.2025.115.13-32

The comparative efficiency and dynamics of the single-sided vibro-impact nonlinear energy sink (SSVI NES) and tuned mass damper (TMD) are shown under periodic excitation with changes in structural parameters. Both SSVI NES and TMD demonstrate fairly high efficiency in mitigating the primary structure vibrations and maintain their tuning.

**Keywords**: nonlinear energy sink, tuned mass damper, vibro-impact, primary structure, efficiency, comparison.

## 1. Introduction

The nonlinear energy sinks (NESs) and the tuned mass dampers (TMDs) are passive vibration control devices. They are designed to mitigate unwanted vibrations in the main structure. This mitigation can be assessed by a reduction of its total mechanical energy, especially in the resonance zone. The difference in the design of NES and TMD lies in the way they are connected to the main structure, which is linear for TMD and nonlinear for NES. The TMDs have been widely discussed in scientific literature and have been implemented in engineering practice. There are several well-known structures in which TMDs were used very successfully.

Scientific literature suggests that NESs, which were proposed two decades ago in frame of the Targeted Energy Transfer (TET) theory, can effectively attennuate the main structure vibrations due to their nonlinearity across a broadband frequency range. The advantage of NES compared with TMD is considered its ability to maintain tuning over a wide range of natural frequencies of the main structure.

Research on both NESs and TMDs, which has been actively conducted for two decades, continues today. Along with comprehensive reviews in recent years [1-5], many new and recent works on NES and TMD research have appeared. There are many studies examining the dynamics of impact-based, i.e. vibro-impact NESs, which are considered as “the most effective NESs for shock and seismic energy absorption and dissipation even at severe loadings” [1]. A number of studies compare the performance of NES and TMD in various specific cases.

In the newest work [6], the authors consider the system, which falls with in the passive control technology; in particular, this system can be seen as an evolution/combination of different passive control systems: tuned mass damper (TMD) systems, particle impact damping systems, and vibro-impact isolation systems. They believe that the tuned mass absorbs the kinetic energy from the main system and dissipate it through the TMD damper and the impacts with the bumpers. Through numerical analyses, an optimal bumper design procedure is introduced. The authors analize, at which conditions the insertion of bumpers can bring significant increses in effectiveness. The scientists of this scientific school also analyze the dynamics of single-degree-of-freedom base-isolated systems whose displacements are limited by optimally designed bumpers [7]. In [8], they use numerical analisys to study the affect of two-sided vibro-impacts on the optimally designed bumpers. The performances of TMD and NES in suppressing vibration in self-excited systems, which vibrate even without external harmonic, is also studied in the latest work [9]. The authors consider their key findings to be assertions that, firstly, a well-designed TMD is highly effective at suppressing vibrations, and, secondly, the NES offers impressive robustness and can expand the range of effective suppression, particularly in systems with external forcing.The paper [10] presents thorough theoretical and numerical investigations of transient dynamics of a linear primary

system coupled with a polynomial stiffness nonlinear vibration absorber (PNVA), which incorporates positive linear and cubic stiffnesses and negative quadratic stiffness. Then, the nonlinear restoring force is a polynomial consisting of linear, quadratic and cubic terms. The comprehensive comparison of the overall performance among the PNVAs, cubic NESs, bistable NESs, and traditional TMDs under free decay vibration induced by different initial conditions allowed the authors to conclude that the "PNVA optimized has the best robustness against structural frequency detuning and relatively good energy dissipation efficiency and robustness against input energy variation". The authors note citing [11] that "in practice, TMDs are often reported to have performance lower than expected". In the paper [12], a two-degree-of-freedom system consisting of a linear oscillator (LO) under harmonic excitation, and an embedded single-sided vibro-impact nonlinear energy sink (SSVI NES) is investigated. Following Hunt and Crossley's model, the authors divide the contact force into two parts: the elastic force and the damping force. They highlight the dependence of the efficiency of energy transfer and dissipation on the changing of SSVI NES parameters and focus on two parameters, the linear stiffness and the loss coefficient of the impact process. They state that the linear stiffness affects the efficiency of energy transfer from the main structure to the SSVI NES, while the loss coefficient determines the efficiency of energy dissipation. We would like to note that the authors point out the difficulty of finding the optimal design for the VI NES and emphasize the great influence of the clearance size. "However, existing NES, including VINES, face the problem of robustness with respect to the vibration level, i.e., the NES is usually effective only in a specific range of moderate vibration amplitudes but fails at high or low vibration levels. From this sense, the effectiveness of a VI NES is very sensitive to its clearance size, making its optimal design a rather challenging issue." The authors of the work [13] also study the effect of different clearances on the response regimes and carry out an optimal anslysis of the stiffness and clearance parameters. They study a system in which a ball in a cavity collides with both its boundaries. The interaction force between the two bodies is generated through equivalent contact stiffness and viscous damping and is written using the Heaviside step function. The effect of clearance of the VI NES on the maximum amplitude and vibration suppression performance of the main linear oscillators is also examined in the paper [14]. This paper presents a comprehensive study of periodically forced, weakly coupled two-degree-of-freedom (2 DOF) linear oscillators integrated with a VI NES. A sweep-frequency analysis is conducted to determine the optimal parameters of the VI NES system across the entire resonance frequency band. It is worth paying attention to article [15] in which, the vibration damping performance of the VI NES for the beam under harmonic force, broadband white noise, and transient shock excitations is discussed and compared to other types of absorbers. The authors claim that non-smooth vibro-impacts allow "a broadband transfer of vibration energy among the eigenmodes of the host beam, resulting in hence a much more effective vibration reduction than the tuned mass damper (TMD) or other NESs". The comparison is made using three examples of the behavior under different excitations. A parametric optimization of the VI NES was conducted concerning the key design parameters: the clearance, the damper location on the beam, and the restitution coefficient. The authors believe that the main parameters that affect the vibration suppression performance of the VI NES are the clearance and the location, but not the vibro-impact damping. The study [16] introduces a novel approach to vibration suppression by integrating a piezoelectric NES with a digitally programmable shunt circuit. An experimental verification conducted to validate the vibration suppression capability of the piezoelectric NES using the test platform confirms the NES performance, showing a significant vibration amplitude reduction in real-world applications. The authors claim that NESs have significant advantages in the broadband control of structural vibrations, but their traditional forms typically involve a large additional mass, complex structural configurations, and difficulties in parameter tuning. The paper [17] experimentally identifies the damping of vertical track NES by appropriately using the restoring force surface method, which is the first reported. The nonlinear damping generated by such factors as friction, prestress, and restraint within the mechanism and its influence on the vibration reduction characteristics is discussed. A multi-frequency harmonic balance method is proposed in the paper [18] in which a mathematical model is established for a rectangular plate with four-point support and a NES under arbitrary multi-frequency excitation. The proposed method validity and high computational precision have been validated through a comparison with numerical results. The possible application of the vibro-impact absorber in practical mechanical engineering is described in [19]. This study introduces a novel, asymmetrically constrained vibro-impact nonlinear energy sink to suppress broadband vibrations induced

by collision and friction in clearance joints. Clearance joints introduce complex nonlinear effects, such as contact collisions, stick-slip friction, and local compliance changes that significantly influence mechanism dynamics. A dedicated experimental platform is developed to investigate the nonlinear vibration in the clearance joint and validate the passive control method. The proposed controller achieves broadband vibration suppression without external energy input by incorporating asymmetric bilateral and vibro-impact interaction. The paper [20] also analyzes the dynamics of vibro-impact system under the presence of dry friction. The system consists of a harmonically excited capsule and a bullet that is freely moving in its interior. The system is non-smooth due to the impacts at the bottom (top) of the capsule. Dry friction introduces a second type of non-smoothness, dynamical system is discontinuous. With harmonic forcing, the system exhibits different types of non-smooth periodic behavior that, due to the dry friction, may include sticking intervals where the capsule and bullet move together.The paper [21] systematically investigates the suppression mechanisms of flow-induced vibration in elastically supported rigid cylinder with an additional NES. Flow-induced vibrations are typical fluid-structure interaction phenomenon observed in slender structures, commonly encountered in marine and civil engineering applications.The results demonstrate that the addition of a weakly nonlinear NES effectively mitigates vibrations of both the circular cylinder and square cylinder, while its effectiveness is significantly diminished in the case of strongly coupled square cylinder.

To summarize these short descriptions of the article, let us pay attention to the following statements that are often encountered. Firstly, when performing optimization procedures, the authors note the significant influence of clearance on the VI NES efficiency. Secondly, the authors note the difficulties in selecting the optimal VI NES design.

This paper is a continuation of the work [22], which examined the preservation of the tuning of light NES and TMD with a mass ratio of 2% when changing such a structural parameter as the PS damping. In this paper, we study how lighter and heavier NESs and TMDs with mass ratio of 2% and 6% maintain their tuning when various structural parameters, namely, the PS damping and stiffness, as well as the exciting force intencity, are changed. Thus, the main objective of this work is to show how the efficiency of the NES and TMD, the optimal design of which has been found for certain values of the structural parameters, changes when the values of these structural parameters change.

This paper is organized as follows.Section 2 develops the mathematical model of the SSVI NES and presents the governing equations. Section 3 describes the efficiency and dynamic behavior of the SSVI NES and TMD with mass ratio of 6%, tuned to different values of the PS damping when varying this parameter. Section 4 demonstrates the performance of the SSVI NES and TMD with mass ratio of 2% and 6% when varying the PS stiffness. Section 5 shows these characteristics when the exciting force intensity, i.e. its amplitude, changes. Finally, Sectin 6 summarizes the main conclusions.

## 2. Model description and governing equations

This paper examines the dynamics of a mechanical system consisting of a heavy primary structure (PS), which is the linear oscillator, and a light attached damper. We consider two types of dampers, namely, a vibro-impact damper, which is a single-sided vibro-impact nonlinear energy sink (SSVI NES), and a linear damper, which is a tuned mass damper (TMD). The selected SSVI NES scheme (Fig. 1) corresponds to the schemes described in many works [23-26]. It is described in detail in Part 1 of this paper [22], but we are forced to repeat this description in order to understand the paper content. The system is under the influence of a harmonic exciting force acting on the PS

$$F(t)=P\cos(\omega t+\varphi_0),\ T=2/\omega. \quad (1)$$

The vibro-impact damper hits the PS directly and the obstacle during movement, but the linear damper does not produce any impacts, which can be achieved in this circuit by using large values for distances $D$ and $C$. In this paper, we compare the efficiency, dynamics, and ability to maintain the tuning of these

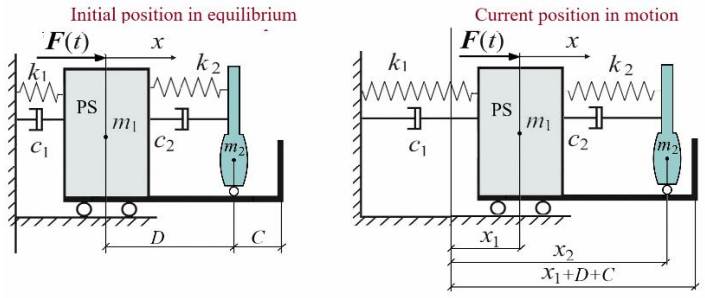


Fig. 1. Conceptual scheme of a single-sided vibro-impact nonlinear sink

ISSN 2410-2547
Опір матеріалів і теорія споруд/Strength of Materials and Theory of Structures. 2025. № 115

dampers when changing structural parameters such as PS damping $c_1$, its stiffness $k_1$, the exciting force intencity, i.e. its amplitude $P$.

The repeated impacts, which occur during movement of the system with attached SSVI NES, are simulated using nonlinear Hertz's contact force according to its quasi-static contact theory [27,28]:

$$F_{con}(z) = K[z(t)]^{3/2}. \tag{2}$$

Here $z(t)$ is the rapprochement of the colliding bodies during an impact; it is defined by the values of coordinates $x_1$ and $x_2$.The relationship between these coordinates also allows us to formulate the Signorini's contact condition for the occurrence of a collision. They are different for impacts on the PS directly and on the obstacle.

$$\begin{aligned} &x_1 \geq x_2, && \text{that is, } x_1 - x_2 \geq 0 \quad \text{for direct impacts on the PS;} \\ &x_2 \geq x_1 + (D+C), && \text{that is, } x_2 - x_1 - (D+C) \geq 0 \quad \text{for impacts on an obstacle.} \end{aligned} \tag{3}$$

So, the colliding body rapprochments during the damper impacts on the PS $z_1$ and on the obstacle $z_2$ looks like this:

$$z_1 = x_1 - x_2, \quad z_2 = x_2 - x_1 - (D+C). \tag{4}$$

The coefficient $K$ in formula (2) characterizes the mechanical and geometric properties of the colliding surfaces and is calculated using the following formula [27]:

$$K_i = \frac{4}{3}\frac{q_i}{(\delta_i + \delta_{i+1})\sqrt{A_i + B_i}}, \quad \delta_i = \frac{1-\nu_i^2}{\pi E_i}, \quad i = 1,3. \tag{5}$$

As there are four colliding surfaces, we have two different values of $K_i$. The Young's moduli of elasticity and Poisson's ratios are the mechanical characteristics of colliding surfaces: $E_1$, $\nu_1$ for the PS surface, $E_3, \nu_3$ for the obstacle surface, $E_2, \nu_2, E_4, \nu_4$ for left and right damper surfaces. The constants $A_i, B_i, q_i$ are joint geometrical characteristics of the colliding surfaces; they are calculated according to the known table [27] depending on the type of contact surfaces. Assuming that both damper surfaces are spherical and PS and obstacle surfaces are flat, then $A_i = B_i = 1/2R_i$, where $R_i$ is the large radius of the damper surface. Assuming that $R_i$ =1°m for both damper surfaces, we set $A_i = B_i = 0.5°\text{m}^{-1}$, $q_i$ =0.319.

Combining the Signorini's contact conditions and the Hertz contact law, and using discontinuous Heaviside step function to "activate" the contact forces, we write down the motion equations for this system in accordance with the fundamental law of dynamics as follows:

$$\begin{aligned} m_1\ddot{x}_1 + c_1\dot{x}_1 + k_1x_1 - c_2(\dot{x}_2 - \dot{x}_1) - k_2(x_2 - x_1 - D) &= F(t) - H(z_1)F_{con}(z_1) + H(z_2)F_{con}(z_2), \\ m_2\ddot{x}_2 + c_2(\dot{x}_2 - \dot{x}_1) + k_2(x_2 - x_1 - D) &= H(z_1)F_{con}(z_1) - H(z_2)F_{con}(z_2). \end{aligned} \tag{6}$$

The initial conditions are:

$$x_1(0) = 0,\ x_2(0) = D,\ \dot{x}_1(0) = \dot{x}_2(0) = 0,\ \varphi_0 = 0.$$

The set of the Ordinary Differential Equations (ODE) (6) is the stiff due to the discontinuous Heaviside step function $H(z)$. It is integrated using the stiff solver *ode23s* from the *Matlab* platform, which provides the variable integration step and make it extremely small at the impact points.

If the damper does not hit either the obstacle or the PS directly, it operates as a linear damper. Equations (6) describe the motion of the system with such a damper if the terms with the contact force are not active. Their activity is controlled by the Heaviside function value, which is determined by the fulfillment or non-fulfillment of the Signorini's contact condition. Therefore, setting large values of distance $D$ and clearance $C$ ensures shockless movement and operation of the damper as Tuned Mass Damper, if its parameters are optimized and tuned to certain structural parameter values.

Both SSVI NES and TMD are used to mitigate the PS vibrations, that is, to reduce the total PS energy. The mechanical total PS energy, as the sum of kinetic and potential energy, is calculated using the well-known formula:

$$E_{1\text{total}}(t) = E_{1\text{kinetic}}(t) + E_{1\text{poten}}(t) = \frac{m_1\dot{x}_1(t)^2 + k_1x_1(t)^2}{2}. \tag{7}$$

Here $x_1(t)$ and $\dot{x}_1(t)$ are obtained by integrating the motion equations (6).

The tuning of dampers consists of selecting a set of optimal parameters that ensure the best mitigation of the PS vibrations. The mitigation of the PS vibrations can be well assessed by the reduction in its maximum mechanical energy. Therefore, it is the maximum PS energy that is chosen as the objective function when performing optimization procedures and selecting the damper optimal design.The analysis of damper efficiency is based on graphs showing changes in maximum PS energy, i.e., using an energy approach.

In this paper, some parameters of the PS and the obstacle are pre-selected

$$1000 \text{ kg}, \ E_1 = E_3 = 2.1 \cdot 10^{11} \text{ N/m}^2, \ \nu_1 = \nu_3 = 0.3.$$

The PS damping $c_1$ and PS stiffness $k_1$, as well as the exciting force amplitude $P$, change; this paper studies how these changes affect the system dynamics and damper efficiency. In our previous works [29], we have found that the softer impacts between the damper and the barriers are preferable and provide the better results, so after optimization we have chosen the following values of Young's moduli and Poisson's ratios for both damper surfaces:

$$E_2 = 2.21 \cdot 10^7 \text{N/m}^2, \ E_4 = 2.05 \cdot 10^7 \text{N/m}^2, \ \nu_2 = \nu_4 = 0.4.$$

### 3. Changing the primary structure damping $c_1$

In [22], the SSVI NESs of mass $m_2$=20 kg coupled to the *PS* were considered under its different damping $c_1$. It was shown that when PS damping $c_1$ is varied, the tendency of non-standard "strange" values of optimal clearance $C$ and damping coefficient $c_2$ for lighter dampers is maintained. It has also been shown that the tuned mass damper demonstrates an effect of mitigating the PS vibrations in the system under consideration, which is as good as the effect exhibited by the vibro-impact nonlinear energy sink for different PS damping $c_1$. In our previous works [30, 31] it was shown that the dynamical behavior of lighter VI NESs differs from that of heavier VI NESs. Therefore, in this section, the SSVI NESs and TMDs of mass $m_2$=60 kg coupled to the PS are considered under its different damping $c_1$. The SSVI NES is tuned for two values of the PS damping $c_1$: $c_1$=452°N·s/m and $c_1$=252 N·s/m. The tuning of the TMD is identical for both these values of $c_1$. In this Section, the PS stiffness is $k_1=3.95 \cdot 10^4$ N/m, and the exciting force amplitude is 800 N.

The *surf* program outputs such values of optimized parameters (Fig. 2).

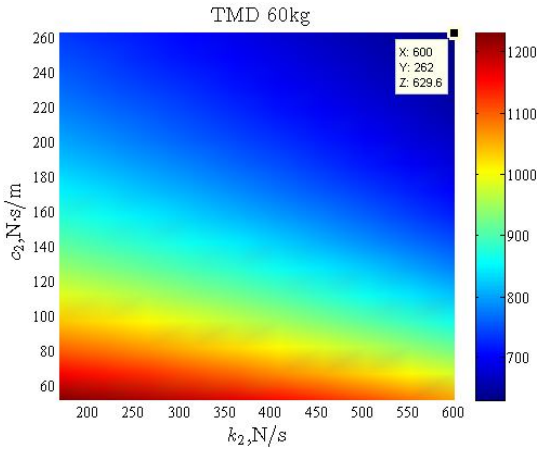


Fig. 2. Finding the optimal parameters of linear TMD using the *surf* program

#### 3.1. Tuning on $c_1$=452 N·s/m

So, the optimized parameter values for the SSVI NES and TMD are as follows:

Table 1

The optimized parameter values for the SSVI NES and TMD when they are tuned to $c_1$=452 N·s/m

| Damper type | $m_2$ , kg | $k_2$ , N/m | $c_2$ , N·s/m | $C$, m | $D$, m |
|---|---|---|---|---|---|
| SSVI NES | 60 | 215 | 232 | 0.360 | 0.0600 |
| TMD | 60 | 600 | 262 | 4.70 | 2.08 |

Large values of distances $C$ and $D$ ensure the motion without impacts, that is, the damper operation as a linear one. Fig. 3 shows the behavior of maximum total energy $E_{1\max}$ of the PS coupled with both SSVI NES and TMD as a function of the exciting force frequency $\omega$ for different values of PS damping $c_1$, smaller and larger than the PS damping $c_1$ at which the dampers were tuned.

Fig. 3 demonstrates high efficiency of both SSVI NES and TMD despite the change in the structural parameter $c_1$. The SSVI NES mitigates the PS vibrations slightly better than the TMD if the PS damping $c_1$ and its value, for which both dampers were tuned, are the same. Both dampers retain their tuning and show the same efficiency when the PS damping $c_1$ is increased (Fig. 3 (b)). But when

ISSN 2410-2547
Опір матеріалів і теорія споруд/Strength of Materials and Theory of Structures. 2025. № 115

the PS damping $c_1$ decreases, the tuning of SSVI NES deteriorates and its efficiency becomes non-uniform at different exciting force frequencies, while the TMD maintains the tuning and uniform efficiency at different exciting force frequencies (Fig. 3 (a)).

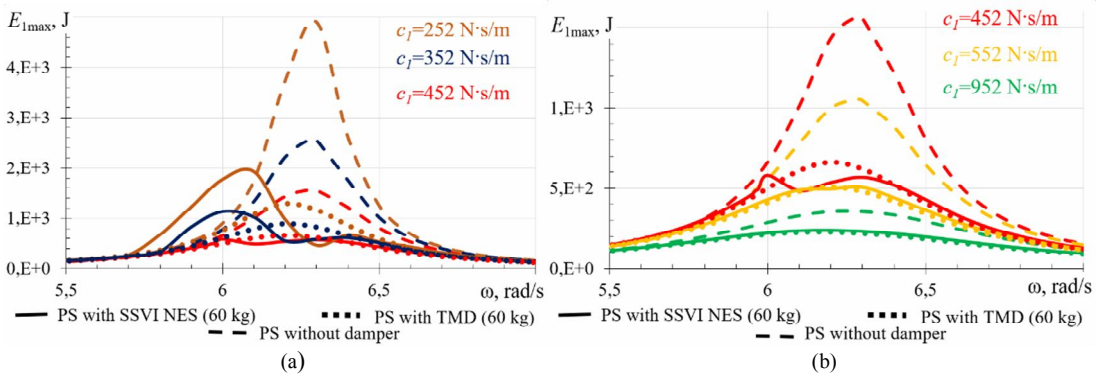


Fig. 3. The reduction of maximum PS energy with attached SSVI NES and TMD with masses $m_2$=60 kg tuned to $c_1$=452 N·s/m when changing the PS damping $c_1$: (a) for $c_1$=252, 352, 452 N·s/m; (b) for $c_1$=452, 552, 952 N·s/m

The maximum PS energy is reduced as the attached damper takes up some of this energy.

Figs. 4, 5 demonstrate clearly this energy transfer for $c_1$ =452 N·s/m. In the left graph, the area of bilateral damper impacts on the PS and obstacle is shown in pink; the areas of unilateral impacts on the PS only are shown in pastel blue. The vertical black straight line shows the resonant frequency.

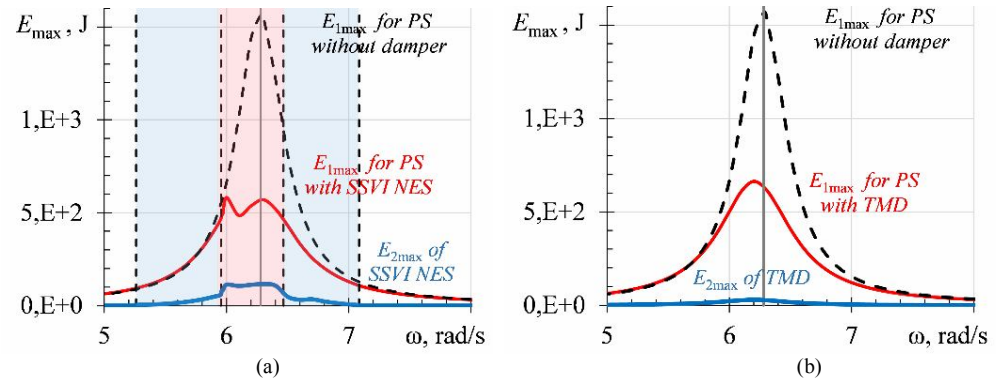


Fig. 4. The zone of bilateral impacts of SSVI NES in pink and the unilateral impacts in blue. The maximum PS energy and the maximum damper energy when PS with $c_1$=452 N·s/m is coupled with dampers also tuned to $c_1$= 452 N·s/m (a) SSVI NES, (b) TMD

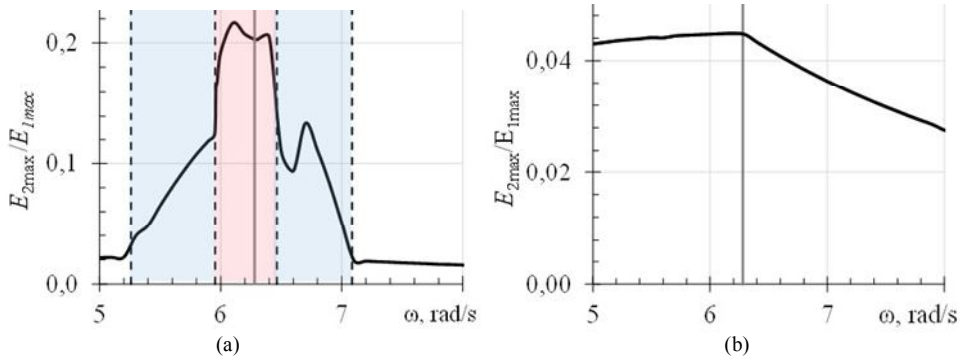


Fig. 5. The relations of the maximum damper energy $E_{2max}$ and the maximum PS energy $E_{1max}$ when PS with $c_1$=452 N·s/m is coupled with dampers also tuned to $c_1$= 452 N·s/m: (a) SSVI NES, (b) TMD

Fig. 5 presents the relations of the maximum damper energy $E_{2\max}$ to maximum PS energy $E_{1\max}$ for the PS with damping $c_1$=452 N·s/m as the functions of the exciting force frequency $\omega$: $E_{2\max}/E_{1\max}$ .

The significantly different appearance of these curves is striking. Although the part of the transferred energy for TMD is much smaller, it reduces the PS energy quite well, which can be clearly seen in Fig. 3.

Similar plots of energy for PS with damping $c_1$=452 N·s/m without damper, the energy $E_1$ of the PS coupled with SSVI NES and TMD also tuned to $c_1$= 452 N·s/m, and damper energy $E_2$ as the functions of time for the resonant exciting force frequency $\omega$=6.28 rad/s are presented in Figs. 6, 7.

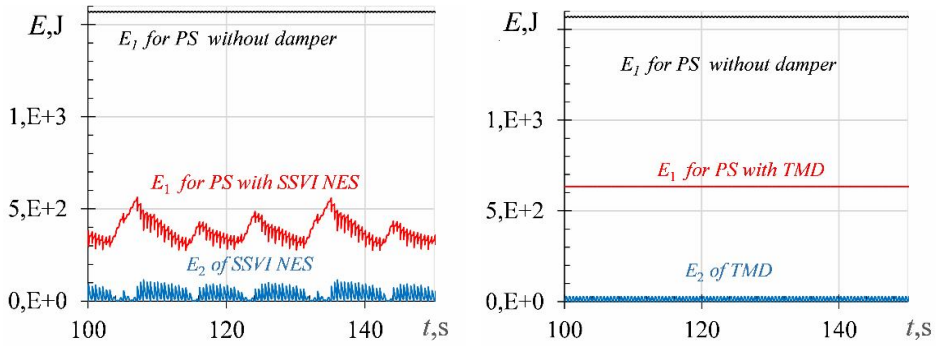


Fig. 6. The PS energy $E_1$ and the damper energy $E_2$ as the functions of time at exciting force frequency $\omega$ =6.28°rad/s when PS with $c_1$ =452 N·s/m is coupled with dampers also tuned to $c_1$= 452 N·s/m: (a) SSVI NES, (b) TMD

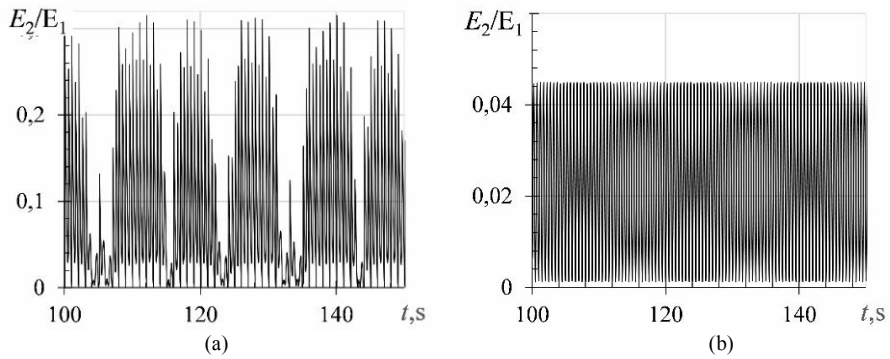


Fig. 7. The relation of the damper energy $E_2$ and the PS energy $E_1$ as the functions of timeat exciting force frequency $\omega$=6.28 rad/s when PS with $c_1$=452 N·s/m is coupled with dampers tuned also to $c_1$= 452 N·s/m: (a) SSVI NES, (b)°TMD

The plots in Fig. 6 again show a slightly better reduction of the PS energy $E_1$ with SSVI NES compared to TMD when the PS damping $c_1$ and its value, for which both dampers were tuned, are the same ($c_1$=452 N·s/m). However, when TMD is coupled to the PS, the energy change over time is smoother.

The graphs in Fig. 7 also show the lower values of the relation $E_2/E_1$ , that is, TMD takes away the smaller part of the PS energy, which does not prevent it from reducing it anyway. The behavior of this relation over time is smoother for TMD.

### 3.2. Tuning on $c_1$=252 N·s/m

Since the TMD tuning is the same for both values of $c_1$=452 N·s/m and $c_1$=252 N·s/m, the optimized parameter values for the SSVI NES and TMD are as follows:

Table 2

The optimized parameter values for the SSVI NES and TMD when they are tuned to $c_1$=252 N·s/m

| Damper type | $m_2$, kg | $k_2$, N/m | $c_2$, N·s/m | $C$, m | $D$, m |
|---|---|---|---|---|---|
| SSVI NES | 60 | 186 | 249 | 0.47 | 0.061 |
| TMD | 60 | 600 | 262 | 4.70 | 2.08 |

ISSN 2410-2547
Опір матеріалів і теорія споруд/Strength of Materials and Theory of Structures. 2025. № 115

Fig. 8 shows in green the behavior of maximum total energy $E_{1max}$ of the PS with damping $c_1$= =252°N·s/m coupled to both SSVI NES and TMD tuned also to $c_1$=452 N·s/m as a function of the exciting force frequency $\omega$. For comparison, the $E_{1max}$ behavior for the PS with damping $c_1$= =252 N·s/m coupled to dampers tuned to PS damping $c_1$=452 N·s/m is shown in black. The green and black dotted curves for PS with attached TMDs tuned to these two different PS damping $c_1$ merge, which means that the TMD holds the tuning well. The black solid curve for the PS with the connected SSVI NES tuned to $c_1$=452 N·s/m is significantly different from the green solid curve for the PS with the connected SSVI NES tuned to $c_1$=252 N·s/m, which means that SSVI NES holds the tuning worse in this case. However, the efficiency of all four dampers is high.

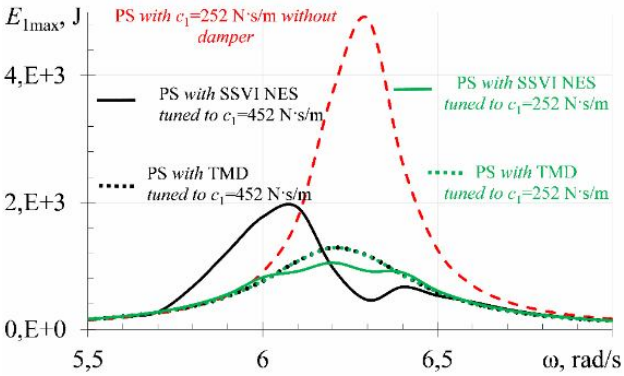


Fig. 8. The reduction of maximum energy of PS with damping $c_1$=252 N·s/m with attached SSVI NES and TMD tuned to two different PS damping $c_1$: green curves to $c_1$=252 N·s/m, black curves to $c_1$=452 N·s/m

Again, as in Fig. 3, the green curves in Fig. 8 show that SSVI NES mitigates the PS vibrations slightly better than the TMD if the PS damping $c_1$ and its value, for which both dampers were tuned, are the same, $c_1$=252 N·s/m in this Fig. But the black curves demonstrate that the reduction of the PS energy coupled with TMD retains the same, while the reduction of the PS energy coupled with SSVI NES becomes very different at different exciting force frequencies when these values are different.

Figs. 9, 10 demonstrate the energy transfer for the PS with damping $c_1$=252 N·s/m. In the left graph, the area of bilateral damper impacts on the PS and obstacle is shown in pink; the areas of unilateral impacts on the PS only are shown in pastel blue. The vertical black straight line shows the resonant frequency.

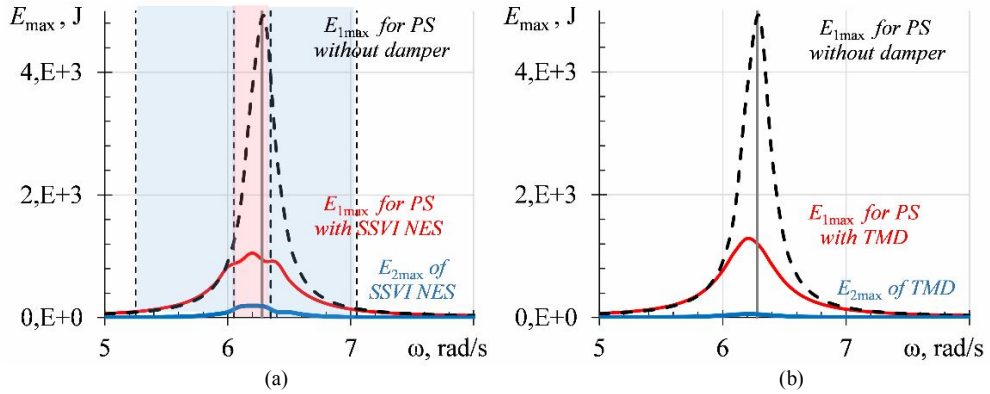


Fig. 9. The maximum PS energy and the maximum damper energy when PS with $c_1$=252 N·s/m is coupled with dampers tuned also to $c_1$= 252 N·s/m (a) SSVI NES, (b) TMD

Fig. 10 presents the relations of the maximum damper energy $E_{2max}$ to maximum PS energy $E_{1max}$ for the PS with damping $c_1$=252 N·s/m as the functions of the exciting force frequency $\omega$: $E_{2max}$ / $E_{1max}$.

Again, as in subsection 3.1, it can be seen that the appearance of these curves is significantly different. Although the part of the transferred energy for TMD is much smaller, it reduces the PS energy quite well, which can be clearly seen in Fig. 8. It should be noted that the ratio $E_{2max}$ / $E_{1max}$ for the PS coupled to the TMD is the same in Fig. 10 and Fig. 5, although the values of $E_{1max}$ and $E_{2max}$ are naturally different when the PS with different damping $c_1$ is coupled to the TMD with the same optimized parameters.

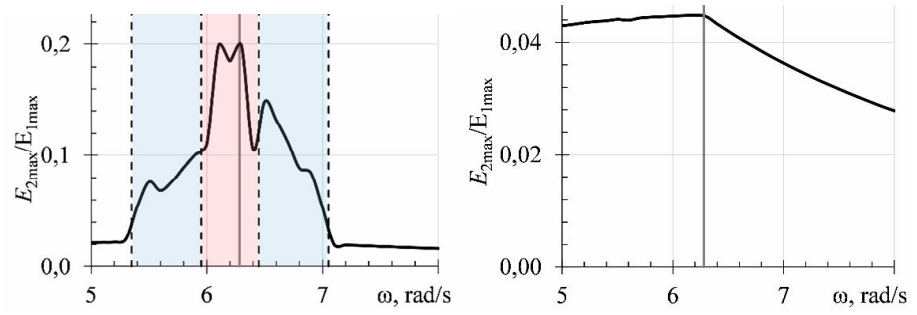


Fig. 10. The relation of the maximum damper energy $E_{2max}$ and the maximum PS energy $E_{1max}$ when PS with $c_1$=252 N·s/m is coupled with dampers tuned also to $c_1$= 252 N·s/m: (a) SSVI NES, (b) TMD

The plots of energy for PS with damping $c_1$=252 N·s/m $E_1$ without damper, the energy $E_1$ of the PS coupled with SSVI NES and TMD tuned also to $c_1$=252 N·s/m, and damper energy $E_2$ as the functions of time for the resonant exciting force frequency $\omega$=6.28 rad/s are presented in Figs. 11, 12.

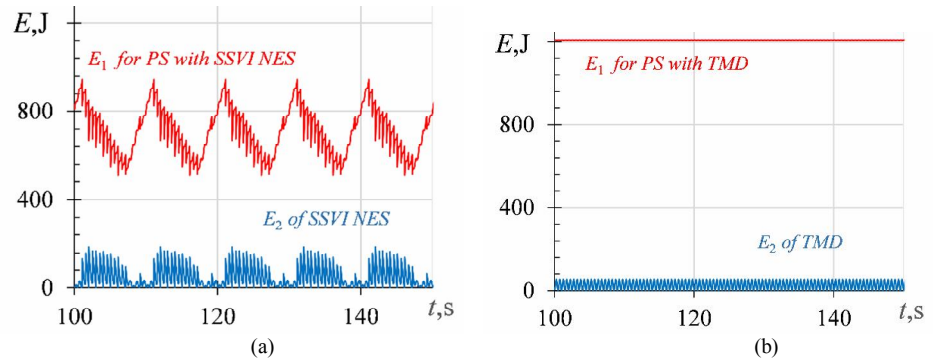


Fig. 11. The PS energy $E_1$ and the damper energy $E_2$ as the functions of time at exciting force frequency $\omega$=6.28°rad/s when PS with $c_1$=252 N·s/m is coupled with dampers tuned also to $c_1$= 252 N·s/m (a) SSVI NES, (b) TMD

The plots in Fig. 11 again show a slightly better reduction of the PS energy $E_1$ in resonant region with SSVI NES compared to TMD when the PS damping $c_1$ and its value, for which both dampers were tuned, are the same ($c_1$=252 N·s/m in this Fig). However, when TMD is coupled to the PS, the energy change over time is smoother.

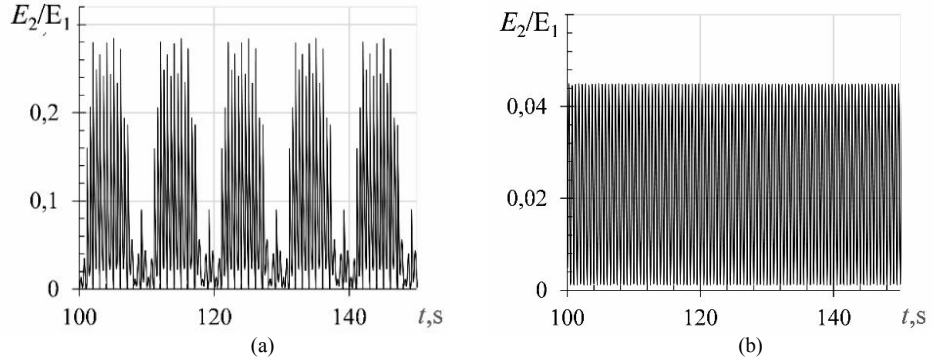


Fig. 12. The relation of the damper energy $E_2$ and the PS energy $E_1$ as the functions of timewhen PS with $c_1$=252°N·s/m is coupled with tuned (a) SSVI NES, (b) TMD

We emphasize that the character of the dependences in Figs. 11 and 12 and in Figs. 6 and 7 does not change; changing the PS damping $c_1$ and the optimal damper design did not affect their character.

ISSN 2410-2547
Опір матеріалів і теорія споруд/Strength of Materials and Theory of Structures. 2025. № 115

### 3.3. Other options of SSVI NES tuned to $c_1$ =252 N·s/m

It is interesting to look at other options for the optimal design of SSVI NES coupled to PS with damping $c_1$=252 N·s/m. The programs *surf* and *fminsearch* allow selecting several different variants of such SSVI NES designs (Fig. 13).

Let's take a look at two of them.

Table 3

The optimized parameter values for the SSVI NESs when they are tuned to $c_1$ =252 N·s/m

| Variant | $m_2$ , kg | $k_2$ , N/m | $c_2$ , N·s/m | $C$, m | $D$, m | $E_{1\max}$ , Jat $\omega$=6.28 rad/s |
|---|---|---|---|---|---|---|
| SSVI NES (V1) | 60 | 170 | 30.0 | 0.500 | 0.0600 | 188.3 |
| SSVI NES (V2) | 60 | 171 | 25.8 | 0.672 | 0.0581 | 1180.6 |

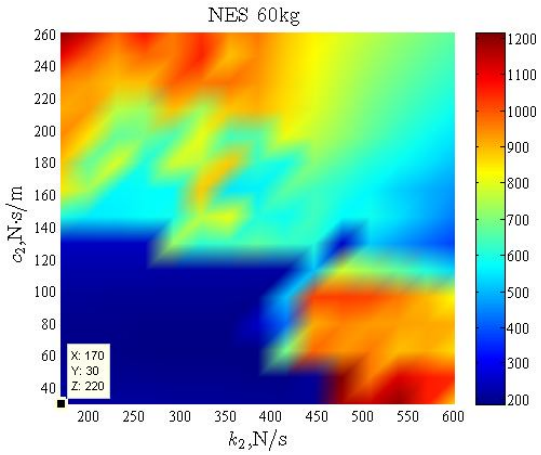


Fig. 13. Finding the optimal parameters of SSVI NES coupled to PS with damping $c_1$=252 N·s/m using the *surf* program

We note the small values of damping coefficient $c_2$ and the PS energy $E_{1\max}$ , i.e., the small value of the objective function,at the resonant frequency. However, the system behavior when the PS is coupled to these SSVI NESs is not similar to that described above. Fig. 14 shows the plots of maximum energy of the PS and SSVI NESs for these two variants as the functions of the exciting force frequency $\omega$, which are significantly different from the plots depicted above. Although the PS energy decreases at the resonant frequency, the resonance peak remains large; it only shifts to the left towards the low frequencies. The PS energy decreases at higher exciting force frequencies, but increases at lower frequencies. The areas of bilateral damper impacts on the PS directly and the obstacle, shown in pink, are much wider; the areas of unilateral direct damper impacts on the PS, shown in pastel blue, are only observed at high and very low frequencies. That is, wide regions of nonlinearity do not provide reliable suppression of the PS vibrations.

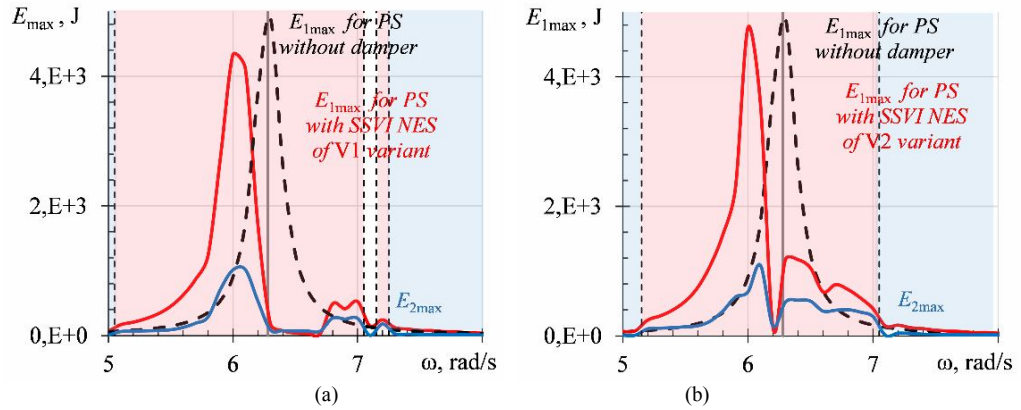


Fig. 14. The zone of bilateral impacts of SSVI NESs in pink and the unilateral impacts in pastel blue. The maximum PS energy and the maximum damper energy when PS with $c_1$=252°N·s/m is coupled with SSVI NESs tuned also to $c_1$= 252 N·s/m: (a) variant V1, (b) variant V2

Fig. 15 presents the relations of the maximum damper energy $E_{2\max}$ to maximum PS energy $E_{1\max}$ for the PS with damping $c_1$=252 N·s/m coupled to SSVI NESs of variants V1 and V2 tuned also to $c_1$=252 N·s/m as the functions of the exciting force frequency $\omega$: $E_{2\max}/E_{1\max}$ . These graphs exhibit

their large values, i.e. the dampers take away a lot of PS energy. However, we see that neither the wide zones of nonlinearity nor the large part of PS energy transferred to the SSVI NES guarantee a sufficiently satisfactory damper efficiency.

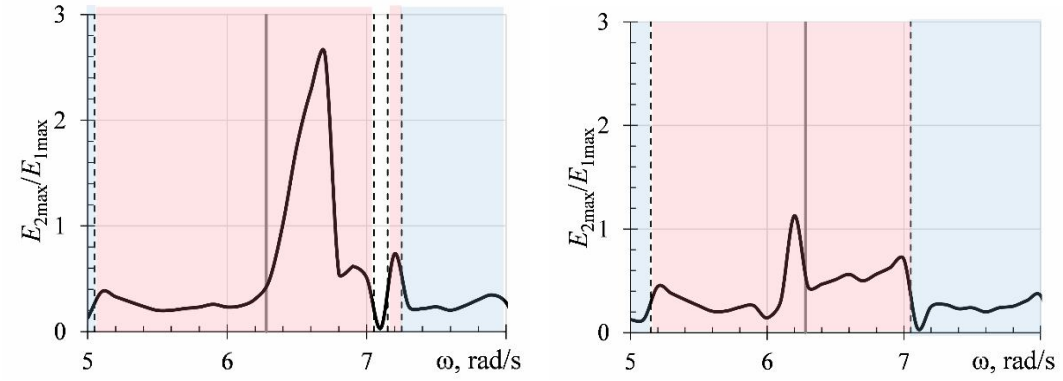


Fig. 15. The relation of the maximum damper energy $E_{2max}$ and the maximum PS energy $E_{1max}$ when PS with $c_1$=252 N·s/m is coupled with SSVI NESs tuned also to $c_1$=252 N·s/m: (a) variant V1, (b) variant V2

Thus, in the case of periodic external load, the TMD demonstrates quite high efficiency in mitigating the PS vibrations and good retention of tuning when such a structural parameter as PS damping $c_1$ is changed. The SSVI NES with optimized parameters also demonstrates high efficiency, in the resonant zone, it can be more effective and stronger to reduce the PS vibrations than TMD, which can be seen in Figs. 3, 6, 8, 11. However, it holds the tuning weaker. Furthermore, finding its optimal deign is a complex and not fully defined, since there are many different parameter sets that provide the similar damper efficiency; and each found design has to be tested.

**4. Changing the primary structure stiffness $k_1$**

The study of the dynamics of the "primary structure – damper" system with a change in the primary structure stiffness $k_1$ exhibits similar results. Naturally, the primary structure natural frequency changes with a change in its stiffness. It is calculated using the well-known formula $\omega_0 = \sqrt{k_1/m_1}$ . This is the resonant frequency of the PS oscillations without any damper. All dampers both SSVI NES and TMD of masses $m_2$ = 20 kg and 60 kg are tuned on stiffness $k_1$ =3.95·10$^4$ N/m and damping $c_1$=452 N·s/m.

The optimized parameters for the SSVI NES and TMD with mass $m_2$=20 kg were given in [22]. Here we repeat them in Table 4 for a more visual representation of all described phenomena.

Table 4

The optimized parameter values for the SSVI NES and TMD of masses $m_2$=20 kg when they are tuned to $k_1$=3.95·10$^4$ N/m and $c_1$=452 N·s/m

| Damper type | $m_2$, kg | $k_2$, N/m | $c_2$, N·s/m | $C$, m | $D$, m |
|---|---|---|---|---|---|
| SSVI NES | 20 | 198 | 36.0 | 0.870 | 0.109 |
| TMD | 20 | 600 | 52.0 | 4.70 | 2.08 |

Dynamic behavior of the maximum PS energy coupled with both SSVI NES and TMD with changing the PS stiffness $k_1$ is shown in Fig. 16. In this Section, the PS damping is $c_1$=452 N·s/m, and the exciting force amplitude is 800 N. The PS energy in the tuned version is shown in red. Naturally, in this case the reduction of the PS energy is maximal. The attached SSVI NES provides two resonance peaks and somewhat better energy reduction than TMD near the resonant frequency. When the PS stiffness changes, both the SSVI NES and the TMD hold their tuning and efficiency and mitigate the PS vibrations quite well. However, the TMD provides somewhat better mitigation. Only at a significantly low stiffness $k_1$=1.00·10$^4$N/m the mitigation is practically absent. The lighter SSVI NES with mass $m_2$ =20 kg does not provide the bilateral impacts on the PS and an obstacle. It only carries out unilateral impacts on the PS directly. The zones of these impacts are shown in Fig. 17 in pastel blue.

ISSN 2410-2547
Опір матеріалів і теорія споруд/Strength of Materials and Theory of Structures. 2025. № 115

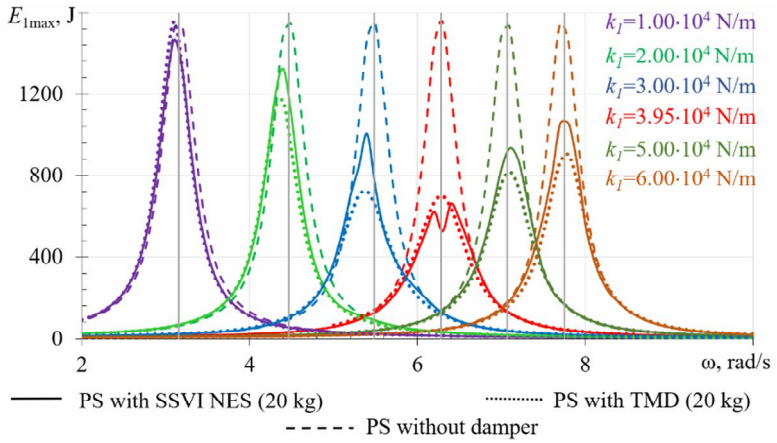


Fig. 16. The reduction of maximum PS energy with attached SSVI NES and TMD of masses $m_2$=20 kg tuned to $k_1$=3.95·10⁴ N/m and $c_1$ =452 N·s/m when changing the PS stiffness $k_1$

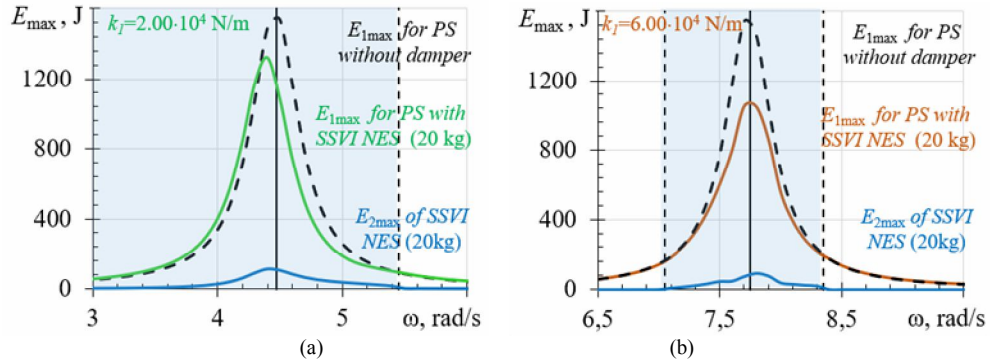


Fig. 17. The zones of unilateral impacts of lighter SSVI NES with $m_2$ =20 kg in blue. The maximum PS energy and the maximum damper energy for two values of the PS stiffness: (a) $k_1$=2.00·10⁴ N/m, (b) $k_1$=6.00·10⁴ N/m

The optimized parameters for the SSVI NES and TMD with mass $m_2$=60 kg were given inTable 1 in Section 3. Fig. 18 shows the dynamic behavior of the maximum PS energy at changing the PS stiffness $k_1$.

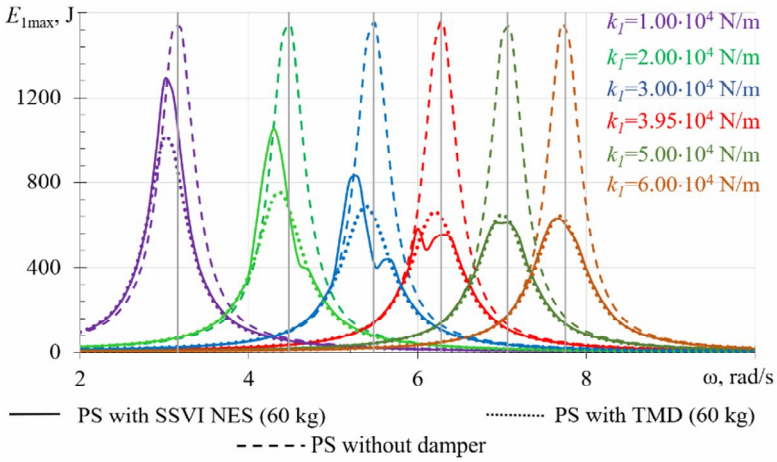


Fig. 18. The reduction of maximum PS energy with attached SSVI NES and TMD of masses $m_2$=60 kg tuned to $k_1$=3.95·10⁴ N/m and $c_1$ =452 N·s/m when changing the PS stiffness $k_1$

In general, the picture for heavier dampers is similar to that shown in Fig. 16. In the version corresponding to the tuning shown in red, the oscillation suppression is achieved best. The SSVI NES provides two resonant peaks and reduces the PS vibrations in the resonance zone somewhat better than TMD. The mitigation is quite good for both the SSVI NES and the TMD at different PS stiffness values. Both damper types retain their tuning, but the TMD retains it somewhat better. However, there are some differences from Fig. 16. With increasing the PS stiffness $k_1$ the energy reduction remains practically unchanged. With decreasing the PS stiffness, the energy reduction worsens, but is maintained even at a significantly low stiffness value.

The heavier damper with mass $m_2$=60 kg realizes bilateral impacts on the PS directly and on the obstacle in the zone shown in Fig. 19 in pink.

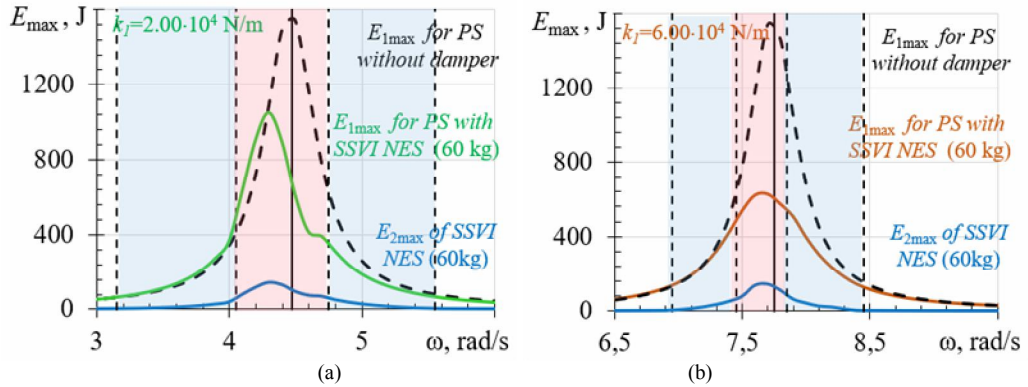


Fig. 19. The zones of bilateral impacts of heavier SSVI NES with $m_2$=60 kg in pink and unilateral impacts on the PS only in blue. The maximum PS energy and the maximum damper energy for two values of the PS stiffness: (a) $k_1$=2.00·10⁴ N/m, (b) $k_1$=6.00·10⁴ N/m

Thus, with periodic excitation, both the SSVI NES and the TMD maintain their tuning and demonstrate high efficiency when changing the PS stiffness $k_1$. The TMD retains its tuning somewhat better, which is especially evident for heavier dampers.

**5. Changing the intensity of the external load *P***

In this section, the SSVI NESs and TMDs of mass $m_2$=20 and 60 kg coupled to the PS are considered under different intensity of the external load, i.e., its amplitude $P$. The SSVI NES and TMD are tuned for two values of the exciting force amplitude $P$: $P$=800 and 3000 N. It was found that the tuning of the TMD is identical for both of these values of $P$, as it is for both values of $c_1$, as shown in Section 3 and in [22]. In this Section, the PS damping is $c_1$=452 N·s/m and PS stiffness is $k_1$=3.95·10⁴ N/m.

**5.1. Tuning on *P*=800 N**

The optimized parameters for the SSVI NES and TMD with mass $m_2$=20 kg are given in Table 4 in Section 4. The optimized parameters for the SSVI NES and TMD with mass $m_2$=60 kg are given in Table 1 in Section 3.

Too large value of the clearance $C$ and small value of the damping coefficient $c_2$ for SSVI NES with mass $m_2$=20 kg are features of lighter vibro-impact dampers. It is these values that provide the best reduction of the PS vibrations. Fig. 20 shows the behavior of maximum total energy $E_{1max}$ of the PS coupled with both SSVI NES and TMD tuned to $P$=800 N as a function of the exciting force frequency $\omega$ for different values of exciting force amplitude $P$. The graphs in Fig.20 are similar to those in Fig. 3, but there are also differences. The SSVI NES with mass $m_2$ of both 20 kg and 60 kg mitigates the PS vibrations near resonance slightly but marginally better than the TMD if the exciting force amplitude $P$ and its value, to which both dampers were tuned, are the same. When the exciting force amplitude increases, both lighter and heavier TMDs hold tuning and maintain uniform high efficiency. But the SSVI NES tuning deteriorates, and its efficiency also deteriorates, which is especially evident at $P$=3000°N. The nature of the system behavior with lighter and heavier dampers is

ISSN 2410-2547
Опір матеріалів і теорія споруд/Strength of Materials and Theory of Structures. 2025. № 115

the same. The only significant difference is that the optimized parameters for the lighter SSVI NES, which ensure such its behavior and efficiency, are non-standard.

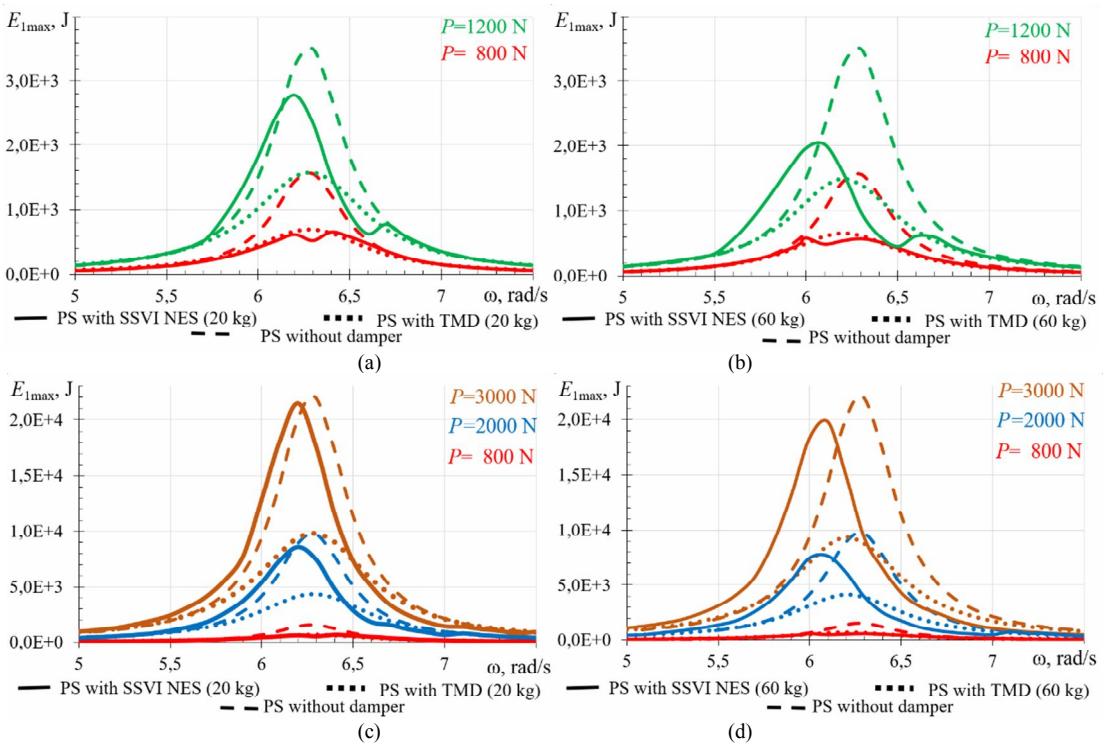


Fig. 20. The reduction of maximum PS energy with attached SSVI NES and TMD of different masses $m_2$, which were tuned to $P$=800 N, when changing the exciting force amplitude: (a) $m_2$=20 kg, $P$=800, 1200 N; (b) $m_2$=60°kg, $P$=800, 1200 N; (c) $m_2$=20 kg, $P$=800, 2000, 3000 N; (d) $m_2$=60 kg, $P$=800, 2000, 3000 N

Energy transfer from the PS to the dampers is shown in Fig. 21 for the system with dampers tuned for $P$=800 N when the exciting force amplitude $P$=1200 N. The areas of nonlinearity for the coupled SSVI NES, in particular the regions of bilateral impacts on the PS directly and on the obstacle, shown in pink, expand as $P$ increases. However, the expansion of nonlinearity zones does not improve the mitigation of the PS vibrations, i.e., the reduction of its energy. The SSVI NES with a larger mass (however, tuned for another $P$=800 N) provide a slightly larger decrease in PS energy. But the resonant peak is shifted and the PS energy at lower frequencies increases. Increasing the TMD mass has little or no effect on its efficiency.

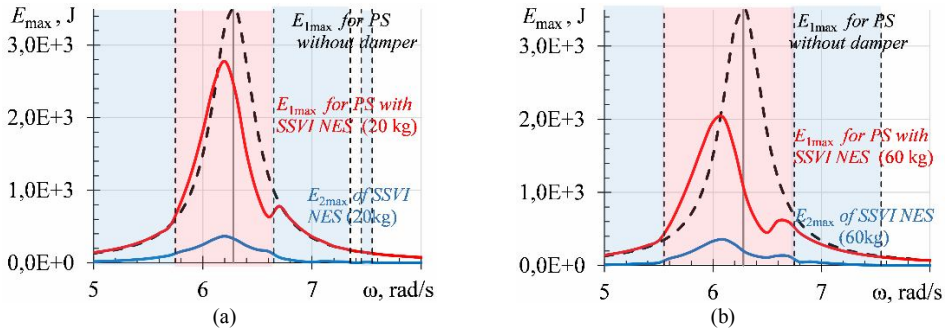


Fig. 21. The maximum PS energy and the maximum damper energy when PS is coupled with SSVI NES and TMD of different masses $m_2$, which were tuned to $P$=800 N, when exciting force amplitude $P$=1200 N: (a) SSVI NES of $m_2$=20 kg, (b) SSVI NES of $m_2$=60 kg

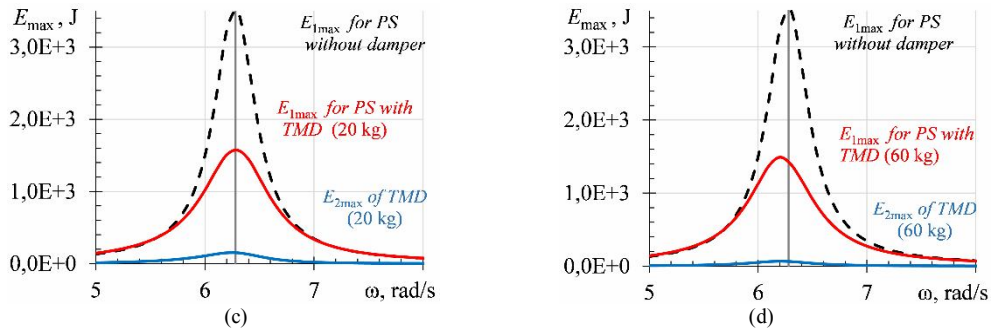


Fig. 21. (continuation). The maximum PS energy and the maximum damper energy when PS is coupled with SSVI NES and TMD of different masses $m_2$, which were tuned to $P$=800 N, when exciting force amplitude $P$=1200 N: (c) TMD of $m_2$=20 kg, (d) TMD of $m_2$=60 kg

The plots of the energy $E_1$ of the PS coupled with SSVI NES and TMD of masses $m_2$=20 kg, tuned to $P$=800 N, and damper energy $E_2$ as the functions of time for the resonant exciting force frequency $\omega$=6.28 rad/s at the exciting force amplitude $P$=1200 kg are presented in Figs. 22.

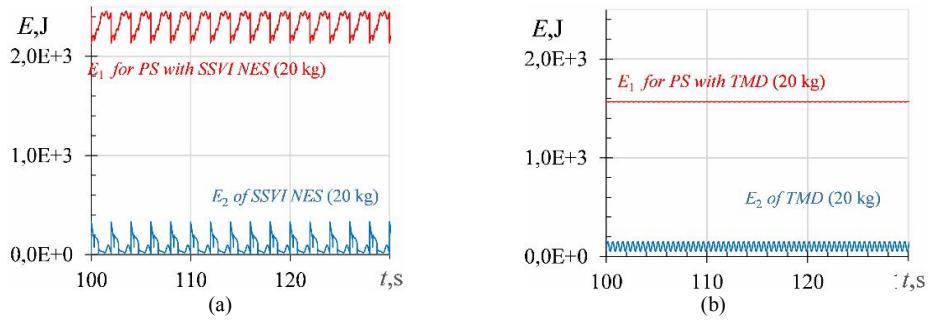


Fig. 22. The PS energy $E_1$ and the damper energy $E_2$ as the functions of time at exciting force frequency $\omega$=6.28°rad/s when PS is coupled with dampers of masses $m_2$=20 kg tuned to $P$=800 N: (a) SSVI NES, (b) TMD

These plots confirm the curves in Fig. 22 (a) and (c) that TMD in this case reduces the PS energy more strongly, despite the smaller values of $E_2$ energy it took away from the PS.

### 5.2. Tuning on $P$=3000 N

Tuning the dampers on large amplitude of the exciting force $P$=3000 N gives the next optimized parameter sets that are presented in Table 5.

Table 5

The optimized parameter values for the SSVI NES and TMD when they are tuned to $P$=800 N

| Damper type | $m_2$, kg | $k_2$, N/m | $c_2$, N·s/m | $C$, m | $D$, m |
|---|---|---|---|---|---|
| SSVI NES (1) | **20** | 200 | 198 | 0.901 | 0.070 |
| (2) | **20** | 100 | 135 | 0.802 | 0.060 |
| (3) | **20** | 150 | 72.8 | 2.10 | 0.100 |
| TMD | **20** | 600 | 52.0 | 4.70 | 2.08 |
| SSVI NES | **60** | 100 | 260 | 0.900 | 0.070 |
| TMD | **60** | 600 | 262 | 4.70 | 2.08 |

Previously, we showed that some optimized parameters for SSVI NES with low mass tend to take non-standard values: the clearance $C$ becomes very large and the damping coefficient $c_2$ too small. Table 5 shows that tuning the SSVI NES with a larger mass to a large exciting force amplitude also yields a large $C$ clearance value. Recall that the large values of $C$ and $D$ for TMD are chosen to ensure the shockless motion and linear operation of the damper. The choice of optimized parameters for the SSVI NES with a smaller mass $m_2$=20 kg when tuned to $P$=3000 kg is ambiguous. Table 5 shows 3 variants of this choice. They show different values of the damper characteristics $k_2$ and $c_2$ and large values of the clearance $C$ for all three

ISSN 2410-2547
Опір матеріалів і теорія споруд/Strength of Materials and Theory of Structures. 2025. № 115

variants. All three damper variants demonstrate a similar efficiency in mitigating the PS vibrations and a similar manifestation of nonlinearity, which will be shown below for the first variant SSVI NES (1).

Table 6

The optimized parameter values for the SSVI NES and TMD with different masses $m_2$ when they are tuned to different exciting force amplitude

| Tuned for | Damper type | $m_2$, kg | $k_2$, N/m | $c_2$, N·s/m | $C$, m | $D$, m |
|---|---|---|---|---|---|---|
| 800 N | TMD | **20** | 600 | 52.0 | 4.70 | 2.08 |
| 3000 N | TMD | **20** | 600 | 52.0 | 4.70 | 2.08 |
| 800 N | TMD | **60** | 600 | 262 | 4.70 | 2.08 |
| 3000 N | TMD | **60** | 600 | 262 | 4.70 | 2.08 |
| 800 N | SSVI NES | **20** | 198 | 36.0 | 0.870 | 0.109 |
| 3000 N | SSVI NES (1) | **20** | 200 | 198 | 0.901 | 0.070 |
| 800 N | SSVI NES | **60** | 215 | 232 | 0.360 | 0.0600 |
| 3000 N | SSVI NES | **60** | 100 | 260 | 0.900 | 0.070 |

Data from Table 1(Section 3), Tables 4 and 5 are summarized in Table 6 to compare the values of damper parameters optimized for different masses and exciting force amplitudes.

Table 6 clearly shows that the tuning of TMD depends only on its mass and is independent of the exciting force amplitude. It was shown in Section 3 and in [22] that the tuning of TMDs with equal masses is identical for different values of PS damping $c_1$. We now see that it is identical for another structural parameter as well. Fig. 23 clearly demonstrates this effect, the appearance of surface projections created by the *surf* program is the same, and the values of parameters in the data-windows are also the same.

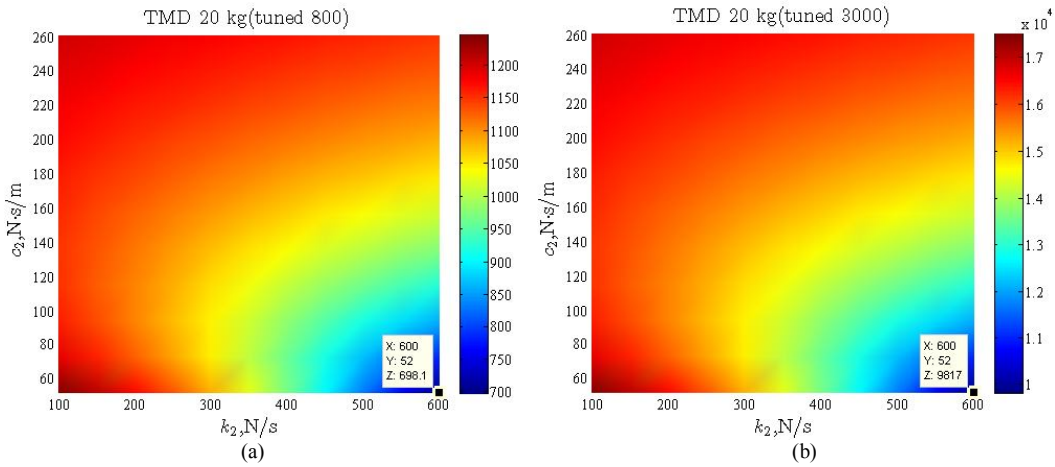


Fig. 23. The relationship between two parameters of TMD of mass $m_2$=20 kg, created with the *surf* program, when they were tuned to different values of exciting force amplitude: (a) $P$=800 N, (b) $P$=3000 N

The dynamic behavior of the maximum PS energy and its reduction when coupling different dampers tuned to $P$=3000 N are shown in Fig. 24.

The graphs for different masses in Fig. 24 do not differ much from each other. The dampers tuned to large exciting force amplitude $P$=3000 kg retain their tuning when exciting force amplitude is reduced. This effect occurs for both TMD and SSVI NES. The efficiency of TMD with $m_2$ =20 kg is significantly higher than that of SSVI NES. The reduction of maximum PS energy by dampers with mass $m_2$=60 kg at different exciting force frequencies is more uniform for TMD than for SSVI NES. Although in some non-broad frequency bands SSVI NES reduces the maximum PS energy more strongly.

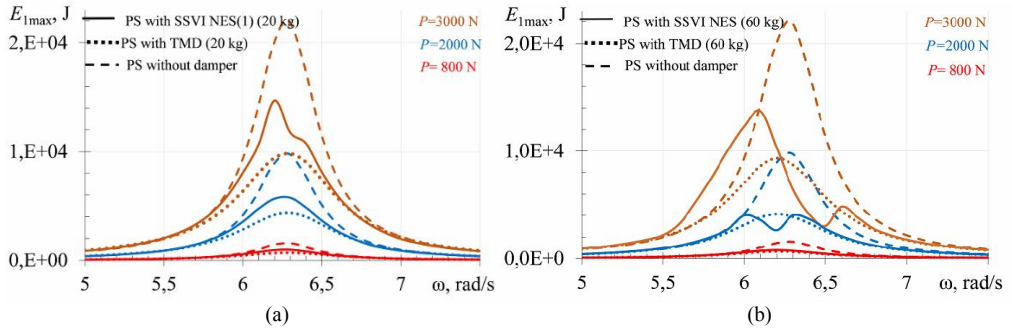


Fig. 24. The reduction of maximum PS energy with attached SSVI NESs and TMDs of different masses tuned to $P$=3000 kg when changing the exciting force amplitude: (a) $m_2$=20 kg; (b) $m_2$=60 kg

The depiction of nonlinearity zones in Fig. 25 gives a varied "motley" picture. If SSVI NES of mass $m_2$=60 kg, tuned to $P$=3000 N, at the exciting force amplitude $P$=3000 N provides quite a wide region of bilateral impacts, shown in pink color, then with decreasing of this amplitude such region decreases and disappears altogether for $P$=800 N. The SSVI NES of mass $m_2$=20 kg, tuned to $P$=3000 N, provides only a narrow region of bilateral impacts even at the exciting force amplitude $P$=3000 N, but it also disappears when this amplitude decreases. The regions of unilateral damper impacts only directly on the PS are shown in blue. However, the presence and breadth of nonlinearity zones, in particular the regions of bilateral damper impacts, do not give a clear picture of the operation and efficiency of the damper. The dynamic behavior of the PS maximum energy shown in Fig. 24 provides a clearer picture of this effect.

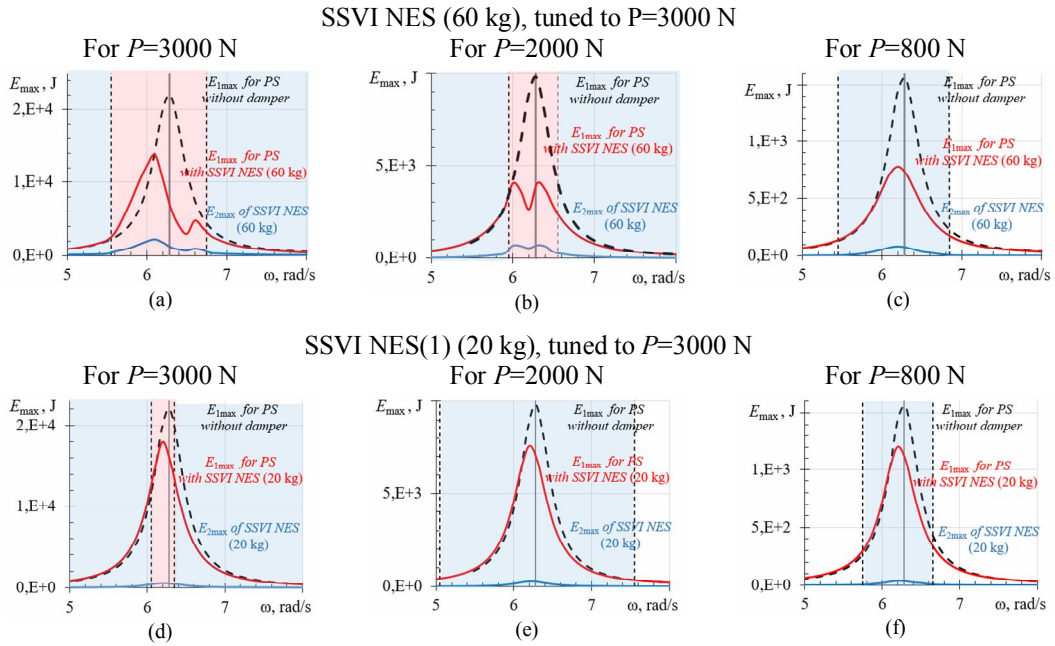


Fig. 25. The zones of bilateral damper impacts in pink and the unilateral impacts in blue. The maximum PS energy and the maximum damper energy when PS is coupled with SSVI NESs of different masses $m_2$, tuned to $P$=3000°N for different values of exciting force amplitude $P$: (a) $m_2$ =60 kg for $P$=3000 N; (b) $m_2$ =60 kg for $P$=2000 N; (c) $m_2$ =60 kg, for $P$=800 N; (d) $m_2$ =20 kg for $P$=3000 N; (e) $m_2$ =20 kg for $P$=2000 N;(f) $m_2$ =20 kg, for $P$=800 N

Thus, the effect of varying such a structural parameter as the intensity of the external load, i.e., the amplitude of the exciting force $P$ in our case, when tuning the SSVI NES and TMD to its different values is similar to the effect of varying the PS damping $c_1$, descripted in Section 3. In the case of periodic external load, both the SSVI NES and the TMD demonstrate quite high efficiency in

mitigating the PS vibrations and good retention of tuning when $P$ is changed, but TMD retains its tuning somewhat better.

**6. Conclusions**

This paper investigates the influence of structural parameter changes on the efficiency and dynamics of the SSVI NES and TMD with optimized design under periodic excitation. The article focused on the ability of these dampers to maintain their tuning. This ability was studied for lighter dampers with a mass ratio of 2% and heavier dampers with a mass ratio of 6% when changing structural parameters such as PS damping, PS stiffness, and the exciting force intencity. It has been convincingly shown that both the SSVI NES and the TMD retain their tuning and demonstrate high efficiency in mitigating the PS vibrations across fairly wide ranges of these parameters. The TMD retains tuning no worse than SSVI NES, and in some cases even better. At the same time, SSVI NES, which always exhibits complex dynamics, provides narrow zones of bilateral damper impacts on the PS directly and on the obstacle located near the resonance. The lighter SSVI NESs exhibit a special behavior. Their high efficiency is ensured by non-standard unusual values of large clearance and small damping coefficient. Furthermore, selecting the optimal SSVI NES design is difficult because there are many sets of optimal parameters that provide their similar performance.

Thus, the advantage of the SSVI NES over the TMD under periodic excitationis not obvious. Therefore, it is necessary to demonstrate this advantage under transient loads, such as impulsive and blast ones, which is included in the author's plans for further work.

REFERENCES

1. Saeed A. S., Abdul Nasar R., Al-Shudeifat M. A. A review on nonlinear energy sinks: designs, analysis and applications of impact and rotary types // Nonlinear Dynamics. – 2022. – T. 111, № 1. – C. 1–37. https://doi.org/10.1007/s11071-022-08094-y
2. Lu Z., Wang Z., Zhou Y., Lu X. Nonlinear dissipative devices in structural vibration control: A review // Journal of Sound and Vibration. – 2018. – T. 423. – C. 18–49. https://doi.org/10.1016/j.jsv.2018.02.052
3. Lu Z., Wang Z., Masri S. F., Lu X. Particle impact dampers: Past, present, and future // Structural Control and Health Monitoring. – 2017. – T. 25, № 1. – C. e2058. https://doi.org/10.1002/stc.2058
4. Wang J., Wierschem N. E., Spencer B. F., Lu X. Track nonlinear energy sink for rapid response reduction in building structures // Journal of Engineering Mechanics. – 2015. – T. 141, № 1. https://doi.org/10.1061/(ASCE)EM.1943-7889.000082
5. Wierschem N. E., Spencer B. F. Jr. Targeted energy transfer using nonlinear energy sinks for the attenuation of transient loads on building structures // Tech. Rep. 045. – Newmark Structural Engineering Laboratory, University of Illinois at Urbana-Champaign, 2015. – https://www.ideals.illinois.edu/items/89701
6. Pagano D., De Angelis M., Andreaus U. Study on the Influence of Impact in Tuned Mass Systems // Earthquake Engineering & Structural Dynamics. – 2025. https://doi.org/10.1002/eqe.70058
7. Perna G., De Angelis M., Andreaus U. Optimal design of single-degree-of-freedom vibro-impact system under harmonic base excitation // https://doi.org/10.21741/9781644902431-70 (accessed: 29.09.2025)
8. Pagano D., Perna G., De Angelis M., Andreaus U. Nonlinear dynamic response of the vibro-impact systems subjected to harmonic ground motion under conditions of uncertainty on the gap size // International Journal of Non-Linear Mechanics. – 2024. – T. 165. – C. 104816. https://doi.org/10.1016/j.ijnonlinmec.2024.104816
9. Chao C., Dai W., Shi B., Branson D., Yang J. Suppression of self-excited vibrations using tuned mass damper or nonlinear energy sink // Nonlinear Dynamics. https://doi.org/10.1007/s11071-025-11769-x
10. Dai X., Wei X., Tang L. Transient dynamics of a polynomial stiffness nonlinear vibration absorber: Theoretical and numerical investigations // International Journal of Non-Linear Mechanics. – 2025. – T. 179. – C. 105242. https://doi.org/10.1016/j.ijnonlinmec.2025.105242
11. Caetano E., Cunha Á., Magalhães F., Moutinho C. Studies for controlling human-induced vibration of the Pedro e Inês footbridge, Portugal. Part 1: Assessment of dynamic behaviour // Engineering Structures. – 2010. – T. 32, № 4. – C. 1069–1081. https://doi.org/10.1016/j.engstruct.2009.12.034
12. Lin Z., Li H., Li A., Zhang Z., Kong X., Ding Q. Dynamic analysis of single-sided vibro-impact nonlinear energy sinks via forced response curves and application to vibration mitigation // Journal of Sound and Vibration. – 2025. – T. 612. – C. 119150. https://doi.org/10.1016/j.jsv.2025.119150
13. Wang Y., Zhang J., Wang W., Wang Z., Hong J., Fang B. Research on the influence of finite contact stiffness on vibration reduction of a vibro-impact nonlinear energy sink system // International Journal of Non-Linear Mechanics. – 2025. – T. 170. – C. 104991. https://doi.org/10.1016/j.ijnonlinmec.2024.104991
14. Fang B., Wang Y.-C., Mao G.-X., Wang W. Vibro-impact nonlinear energy sink dynamics in a harmonically excited weakly coupled two-degree-of-freedom linear oscillator // Chaos, Solitons & Fractals. – 2025. – T. 199. – C. 116670. https://doi.org/10.1016/j.chaos.2025.116670
15. Zhang B., Zhang Z., Jiang J., Zhang Y., Li B., Li H., Xian H. Advantages of vibro-impact nonlinear energy sinks for vibration suppression of continuous systems: Coexistence of inter-modal energy scattering and targeted energy transfer //

Communications in Nonlinear Science and Numerical Simulation. – 2025. – T. 151. – C. 108993. https://doi.org/10.1016/j.cnsns.2025.108993
16. Zhong Y., Fang Y., Dekemele K., Ma X., Zhang Z. Vibration suppression using a programmable piezoelectric nonlinear energy sink // International Journal of Mechanical Sciences. – 2025. – T. 303. – C. 110626. https://doi.org/10.1016/j.ijmecsci.2025.110626
17. Li S.-B., Ding H., Jing X. Identification and influence of cubic nonlinear damping of vertical track nonlinear energy sinks // Mechanical Systems and Signal Processing. – 2025. – T. 238. – C. 113164. https://doi.org/10.1016/j.ymssp.2025.113164
18. Mao X.-Y., Wu J.-B., Zhang J.-N., Ding H., Chen L.-Q. Vibration control of NES for point-supported plate under arbitrary multi-frequency excitation // Communications in Nonlinear Science and Numerical Simulation. – 2025. – T. 148. – C. 108863. https://doi.org/10.1016/j.cnsns.2025.108863
19. Wu X., Li G., Sun Y., Wang H., Chen Y. Theoretical and experimental exploration on the chattering control for the planar mechanism with clearance joint: using an asymmetrically constrained vibro-impact absorber // Mechanism and Machine Theory. – 2025. – T. 215. – C. 106171. https://doi.org/10.1016/j.mechmachtheory.2025.106171
20. Athanasouli C., Yurchenko D., Kuske R. Analysis of Dry Friction Dynamics in a Vibro-Impact Energy Harvester // arXiv. – 2025. – arXiv:2502.12288. https://doi.org/10.48550/arXiv.2502.12288
21. Huang Z., Wang J., Zhang D., Wang X. Investigation of vibration suppression by nonlinear energy sink (NES) based on structure–wake oscillator coupled model // International Journal of Non-Linear Mechanics. – 2025. – T. 178. – C. 105219. https://doi.org/10.1016/j.ijnonlinmec.2025.105219
22. Lizunov P., Pogorelova O., Postnikova T. Tuning of vibro-impact nonlinear energy sinks under changing structural parameters // Strength of Materials and Theory of Structures. – 2025. – T. 114. – C. 11–22. https://doi.org/10.32347/2410-2547.2025.114.11-22
23. Wierschem N. E., Hubbard S. A., Luo J., Fahnestock L. A., Spencer B. F., McFarland D. M., Quinn D. D., Vakakis A. F., Bergman L. A. Response attenuation in a large-scale structure subjected to blast excitation utilizing a system of essentially nonlinear vibration absorbers // Journal of Sound and Vibration. – 2017. – T. 389. – C. 52–72. https://doi.org/10.1016/j.jsv.2016.11.003
24. Li T., Seguy S., Berlioz A. On the dynamics around targeted energy transfer for vibro-impact nonlinear energy sink // Nonlinear Dynamics. – 2016. – T. 87, № 3. – C. 1453–1466. https://doi.org/10.1007/s11071-016-3127-0
25. AL-Shudeifat M. A., Wierschem N., Quinn D. D., Vakakis A. F., Bergman L. A., Spencer B. F. Numerical and experimental investigation of a highly effective single-sided vibro-impact non-linear energy sink for shock mitigation // International Journal of Non-Linear Mechanics. – 2013. – T. 52. – C. 96–109. https://doi.org/10.1016/j.ijnonlinmec.2013.02.004
26. Li W., Wierschem N. E., Li X., Yang T. On the energy transfer mechanism of the single-sided vibro-impact nonlinear energy sink // Journal of Sound and Vibration. – 2018. – T. 437. – C. 307–323. https://doi.org/10.1016/j.jsv.2018.08.057
27. Johnson K. L. Contact Mechanics. – Cambridge: Cambridge University Press, 1985.
28. Goldsmith W. The Theory and Physical Behaviour of Colliding Solids. – London: Edward Arnold Publishers Ltd, 1960.
29. Lizunov P., Pogorelova O., Postnikova T. Optimization of a vibro-impact damper design using MATLAB tools // Strength of Materials and Theory of Structures. – 2024. – T. 112. – C. 3–18. https://doi.org/10.32347/2410-2547.2024.112.3-18
30. Lizunov P., Pogorelova O., Postnikova T. Influenceofstiffnessparametersonvibro-impactdamperdynamics // *StrengthofMaterialsandTheoryofStructures*. – 2023. – No. 110. – P. 21–35. – DOI: 10.32347/2410-2547.2023.110.21-35
31. Lizunov P., Pogorelova O., Postnikova T. Thesynergisticeffectofthemultipleparametersofvibro-impactnonlinearenergysink // *JournalofAppliedMath*. – 2023. – Vol. 1, No. 3. – P. 199. – DOI: 10.59400/jam.v1i3.199

*Стаття надійшла 29.09.2025*

*Лізунов П.П., Погорелова О.С., Постнікова Т.Г.*

**НАЛАШТУВАННЯ ВІБРОУДАРНИХ НЕЛІНІЙНИХ ПОГЛИНАЧІВ ЕНЕРГІЇ ПРИ ЗМІНІ КОНСТРУКТИВНИХ ПАРАМЕТРІВ. ЧАСТИНА 2. ПОРІВНЯННЯ З ДЕМПФЕРОМ З НАЛАШТОВАНОЮ МАСОЮ.**

У цій статті досліджується динаміка та ефективність пом'якшення коливань первинної конструкції (PS) з використанням одностороннього віброударного нелінійного поглинача енергії (SSVI NES) та демпфера з налаштованою масою (TMD). Розглядається PS, з'єднана з віброударними та лінійними демпферами з масовим співвідношенням 2% та 6% під періодичним збудженням зі зміною структурних параметрів, таких як демпфірування PS, її жорсткість та інтенсивність збуджуючої сили. У статті зосереджено увагу на здатності цих демпферів зберігати свою налаштованість. Численні чисельні експерименти, результати яких відображені у виразних графіках і таблицях, переконливо показують, що як SSVI NES, так і TMD зберігають свою налаштованість і демонструють високу ефективність у зменшенні коливань PS у досить широкому діапазоні цих параметрів. TMD зберігає налаштованість не гірше, ніж SSVI NES, а в деяких випадках навіть краще. Водночас SSVI NES, який завжди демонструє складну динаміку, забезпечує вузькі зони двостороннього ударів демпфера безпосередньо на PS і на перешкоду, які розташовані поблизу резонансу. Легші SSVI NES демонструють особливу поведінку. Їхня висока ефективність забезпечується нестандартними незвичними значеннями великого зазору і малого коефіцієнта демпфірування. Крім того, вибір оптимальної конструкції SSVI NES ускладнюється тим, що існує багато наборів оптимальних параметрів, які забезпечують їхню схожу продуктивність.

Для оцінки зменшення вібрацій PS використовується енергетичний підхід, тобто критерієм зменшення вважається зниження максимальної механічної енергії PS. Показано енергію демпферів, яка відбирається від енергії PS. Зони нелінійності для SSVI NES включають зони двосторонніх та односторонніхударів демпферів на PS та перешкоду; ці зони також показані. Також показані характеристики нерегулярного руху SSVI NES.

**Ключові слова:** нелінійний поглинач енергії, демпфер з налаштованою масою, віброудар, первинна структура, ефективність, порівняння.

*Lizunov P.P., Pogorelova O.S., Postnikova T.G.*
**TUNING OF VIBRO-IMPACT NONLINEAR ENERGY SINKS UNDER CHANGING STRUCTURAL PARAMETERS.PART 2. COMPARISON WITH TUNED MASS DAMPERS**

This paper studies the dynamics and efficiency in mitigating the primary structure (PS) vibrations with using the single-sided vibro-impact nonlinear energy sink (SSVI NES) and tuned mass damper (TMD). It is considered the PS coupled with vibro-impact and linear dampers with mass ratio of 2% and 6% under periodic excitation with change in structural parameters such as the PS damping, its stiffness, and exciting force intencity. The paper focuses on the ability of these dampers to maintain their tuning. The numerous numerical experiments, which results are reflected in expressive graphs and tables, convincingly show that both the SSVI NES and the TMD retain their tuning and demonstrate high efficiency in mitigating the PS vibrations across fairly wide ranges of these parameters. The TMD retains tuning no worse than SSVI NES, and in some cases even better. At the same time, SSVI NES, which always exhibits complex dynamics, provides narrow zones of bilateral damper impacts on the PS directly and on the obstacle located near the resonance. Thelighter SSVI NESsexhibit a specialbehavior. Their high efficiency is ensured by non-standard unusual values of large clearance and small dampingcoefficient. Furthermore, selecting the optimal SSVI NES design difficult because there are many sets of optimal parameters that provide their similar performance.

The energy approach is used to estimate the mitigation of PS vibrations, that is, the reduction of maximum mechanical energy of the PS is considered as criterion of mitigation. The energy of dampers, which is taken away from the PS energy, is shown. The zones of nonlinearity for SSVI NES include the zones of bilateral and unilateral damper impacts on the PS and obstacle; these zones also are shown. The characterisitics of irregular motion of SSVI NES are also shown.

**Keywords**: nonlinear energy sink, tuned mass damper, vibro-impact, primary structure, efficiency, comparison.

УДК 539.3
*Лізунов П.П., Погорелова О.С., Постнікова Т.Г.* **Налаштування віброударних нелінійних поглиначів енергії при зміні конструктивних параметрів. Частина 2. Порівняння з демпфером з налаштованою масою** // Опір матеріалів і теорія споруд: наук.-тех. збірн. – К.: КНУБА. 2025. – Вип. 115. – С. 13-32. – Англ.
Порівняльні ефективність та динаміка одностороннього віброударного нелінійного поглинача енергії (SSVI NES) і налаштованого демпфера маси (TMD) показані при періодичному збудженні зі змінами структурних параметрів. Як SSVI NES, так і TMD демонструють досить високу ефективність у зменшенні вібрацій основної конструкції і зберігають свою настройку.
Табл. 5. Іл. 25. Бібліог. 31 назв.

UDC 539.3
*Lizunov P.P., Pogorelova O.S., Postnikova T.G.* **Tuning of vibro-impact nonlinear energy sinks under changing structural parameters.Part 2. Comparison with tuned mass dampers** // Strength of Materials and Theory of Structures: Scientific-and-technical collected articles. – K.: KNUBA. 2025. – Issue115. – P. 13-32.
The comparative efficiency and dynamics of the single-sided vibro-impact nonlinear energy sink (SSVI NES) and tuned mass damper (TMD) are shown under periodic excitation with changes in structural parameters. Both SSVI NES and TMD demonstrate fairly high efficiency in mitigating the primary structure vibrations and maintain their tuning.
Tabl. 5. Figs.25. Refs.31.

**Автор (науковий ступінь, вчене звання, посада)**: доктор технічних наук, професор, завідувач кафедри будівельної механіки КНУБА, директор НДІ будівельної механіки ЛІЗУНОВ Петро Петрович
**Адреса робоча:** 03680 Україна, м. Київ, проспект Повітряних Сил 31, Київський національний університет будівництва і архітектури
**Робочий тел.:** +38(044) 245-48-29
**E-mail:** lizunov@knuba.edu.ua
**ORCIDID:** http://orcid.org/0000-0003-2924-3025

**Автор (науковий ступінь, вчене звання, посада)**: кандидат фізико-математичних наук, старший науковий співробітник, провідний науковий співробітник НДІ будівельної механіки КНУБА ПОГОРЕЛОВА Ольга Семенівна
**Адреса робоча:** 03680 Україна, м. Київ, проспект Повітряних Сил 31, Київський національний університет будівництва і архітектури
**Робочий тел.:** +38(044) 245-48-29
**E-mail:** pogos13@ukr.net
**ORCID ID:** http://orcid.org/0000-0002-5522-3995

**Автор (науковий ступінь, вчене звання, посада)**: кандидат технічних наук, старший науковий співробітник, провідний науковий співробітник НДІ будівельної механіки КНУБА ПОСТНІКОВА Тетяна Георгіївна
**Адреса робоча:** 03680 Україна, м. Київ, проспект Повітряних Сил 31, Київський національний університет будівництва і архітектури
**Робочий тел.:** +38(044) 245-48-29
**E-mail:** postnikova.tg@knuba.edu.ua
**ORCID ID:** https://orcid.org/0000-0002-6677-4127